


Encapsulated papillary carcinoma of the breast: does it have a native basement membrane?

Suzan F Ghannam,^{1,2,3}  Catrin S Rutland,⁴ Cinzia Allegrucci,^{3,4} Nigel P Mongan^{4,5} & Emad Rakha^{1,3}

¹Division of Cancer and Stem Cells, School of Medicine, The University of Nottingham, Nottingham, UK, ²Department of Histology and Cell Biology, Faculty of Medicine, Suez Canal University, Ismailia, Egypt, ³Nottingham Breast Cancer Research Centre, Biodiscovery Institute, University of Nottingham, ⁴School of Veterinary Medicine and Sciences, University of Nottingham, Nottingham, UK and ⁵Department of Pharmacology, Weill Cornell Medicine, New York, NY, USA

Date of submission 22 November 2022
Accepted for publication 1 May 2023

Ghannam S F, Rutland C S, Allegrucci C, Mongan N P & Rakha E

(2023) *Histopathology*. <https://doi.org/10.1111/his.14939>

Encapsulated papillary carcinoma of the breast: does it have a native basement membrane?

Background: Encapsulated papillary carcinoma (EPC) is surrounded by a thick fibrous capsule-like structure, which is interpreted as a thickened basement membrane (BM). This study aimed to describe the geometric characteristics of the EPC capsule and to refine whether it is an expansion of the BM or a stromal reactive process.

Material and Methods: In all, 100 cases were divided into four groups: EPC, ductal carcinoma *in situ* (DCIS), normal breast tissue and invasive tumours, with an additional encapsulated papillary thyroid carcinoma (EPTC) control group. Representative slides from each case were stained with picrosirius red (PSR) stain and examined using polarised microscopy. Images were analysed using ImageJ, CT-FIRE, and Curve align image analysis programmes.

Results: Compared to the normal and DCIS BM, the EPC group showed a significant increase of collagen fibre width, straightness, and density, and a decrease of fibre length. The EPC capsule showed less alignment of fibres with a more perpendicular arrangement, and it was enriched with disorganised collagen

type I (stromal collagen) fibres. Compared to other groups, the EPC capsule showed significant variation in the thickness, evenness, distribution of collagen fibres, and significant intracapsular heterogeneity. Compared to BM-like material in the invasive group, the EPC capsule showed a higher density of collagen fibres with longer, straighter, and more aligned fibres, but there was no difference in the distribution of both collagen types I and III. Conversely, compared to EPTC, there were no differences between both EPC and EPTC capsules except that the fibres in the EPC capsule were straighter. Although differences between normal ducts and lobules and DCIS BM collagen fibre density, straightness, orientation, and alignment were detected, both were significantly different from EPC capsule.

Conclusion: This study provided evidence that the EPC capsule is a reactive process rather than a thickened native BM characteristic of normal and *in situ* lesions, which provides further evidence that EPC is an indolent invasive carcinoma based on capsule characteristics.

Keywords: basement membrane (BM), breast cancer, collagen, Encapsulated papillary carcinoma (EPC)

Address for correspondence: E Rakha, Department of Histopathology, Nottingham University Hospital NHS Trust, City Hospital Campus, Hucknall Road, Nottingham NG5 1PB, UK.
e-mail: mrzear1@exmail.nottingham.ac.uk

Introduction

Papillary lesions of the breast are a heterogeneous group of tumours characterised morphologically by the presence of fibrovascular cores covered by

epithelial cells ranging from benign to malignant.¹ Papillary carcinomas (PCs) include encapsulated papillary carcinoma (EPC), solid papillary carcinoma (SPC), papillary ductal carcinoma *in situ* (DCIS), and invasive papillary carcinoma.^{1,2} EPC typically present as well-circumscribed and encapsulated mass(es) that lack a myoepithelial cell (MEC) layer at their periphery in 80% of cases.³ EPC is a term that has been introduced to define the previously called intracystic or encysted variant of PC to reflect its encapsulation.³ EPC exhibits a peripheral thick capsule-like structure, which was interpreted as a thickened basement membrane (BM) as it contains some of the BM structures, namely laminin and collagen type IV. Subsequently, this feature was used as one of the indications of its *in situ* nature.⁴

BM is a thin, pliable sheet-like material of extracellular matrix (ECM) that sits between normal or proliferative intraductal epithelial and MEC and the surrounding connective tissue.⁵ In malignant tumours, preservation of BM denotes *in situ* disease, while its absence is a feature of invasive tumours.⁵

Although some DCIS shows expansion of the BM, this is different from the reactive fibrous tissue capsule seen around some benign and malignant tumours in various tissue and organs including renal cell carcinomas, hepatocellular carcinomas and thyroid follicular carcinomas, and their benign counterparts.⁶ Tumour encapsulation refers to the presence of a fibrous capsule surrounding the neoplasm and is often associated with indolent clinical behaviour.⁶ The concept of capsule pathogenesis suggests that tumour encapsulation is not a passive condensation of fibrous tissue by expansive growth or a body defence mechanism against tumours as a foreign body response, but is a biological process resembling wound-healing responses.^{6,7}

The World Health Organization (WHO) recommend that EPC are staged as carcinoma *in situ* (pTis) in cases where there is an absence of frank stromal invasion or infiltrative growth despite the lack of an MEC layer.⁸ This was supported by some previous studies showing expression of some BM structures, such as laminin and collagen type IV in EPC, and inferred that the structure around EPC represents expansion of the BM, and hence the intraductal nature of the tumour.^{1,9}

The outer layer of the BM that faces the ECM is called the reticular lamina, or lamina fibro-reticularis, and is mainly formed of collagen III.⁵ Previous studies have demonstrated that collagen III coexpressed with collagen I, resulting in regulation of fibrils dimensions that influence their mechanical stiffness

and functional properties.^{10,11} Collagen III has a key role in normal tension maintenance and modulating scar formation.¹⁰ In addition, BM stiffening has been reported to trigger cell invasiveness in prostate cancer¹² and squamous cell carcinoma.¹³

Picrosirius red (PSR) stain is a special histochemical stain for collagen. PSR has a higher specificity for collagen fibre detection compared to other commonly used stains, as it can stain finer collagen fibrils, which in turn avoids underestimation of collagen density.¹⁴ PSR is comprised of elongated birefringent dye molecules that can bind to the collagen fibres in parallel positions to the fibres, thus improving the natural birefringence under a polarizing microscope. It therefore detects thinner fibres (type III collagen) that are visualised as green to greenish yellow colours, while thicker fibres (type I collagen) present as yellowish orange to orange red colours.^{15,16}

Therefore, the aim of this study was to ascertain whether the EPC capsule represents a reactive process similar to that seen in some invasive tumours, or an expansion of the native BM mimicking that is seen in some cases of DCIS, and hence explain the intraductal nature of the tumour on the basis of BM geometric characteristics.

Material and Methods

STUDY COHORT

This study included 100 cases of normal and neoplastic breast tissue from patients who presented to Nottingham City Hospital, Nottingham, UK between 1999 and 2006. The cases were divided into four groups, each containing 25 patients. The four groups included encapsulated papillary carcinoma (EPC), in addition to ductal carcinoma *in situ* (DCIS), normal breast tissue, and invasive carcinoma (INV) as control groups. The INV group included adenoid cystic carcinoma, invasive cribriform, and salivary gland-like carcinoma, as these meet the criteria of being aggressive tumours and showed BM-like material surrounding the neoplastic cells. Encapsulated papillary thyroid carcinoma (EPTC) cases were also stained and analysed for comparison against the EPC capsule group and used as a control group.

TISSUE PROCESSING AND STAINING

Freshly cut, 4- μ m thick, full-face sections for the cohort were stained with haematoxylin and eosin (H&E) or picrosirius red (PSR) special stain; one section per case from each tumour block was prepared

using each stain. Collagen fibres were assessed using tissue sections stained with PSR. A preparation of PSR solution was undertaken by mixing 200 mg of Sirius Red (Direct red 80, lot#MKCJ4451, 365548, Sigma-Aldrich, Darmstadt, Germany) into 200 ml of saturated aqueous solution of picric acid 2.1% (lot://7883, RRSP143-E, Atom-Scientific, Hyde, England). A liver tissue section was used as a positive control. Sections were deparaffinised, rehydrated, immersed in the picrosirius red solution for 60 min, rinsed twice in acidified water, then dehydrated in 100% ethanol.

MICROSCOPY AND IMAGING

H&E-stained slides were examined, via standard light microscopy with a 10× objective, for histopathological verification of the section. The glands were identified that served as a reference once the tissue sections had been stained with PSR.

The PSR-stained tissue was examined under polarised microscope and visualised using the accompanying software (Leica, IL 5000B, and LAS VER-SION 3.8.0, Leica Microsystems, Switzerland) and a camera. Under polarised light, PSR-stained collagen type I presents within the red-orange-yellow range and type III as green; under light microscopy, total collagen can be visualised within the red spectrum and the two collagen types cannot be differentiated.¹⁷ Tissue sections were split into four quadrants. From each quadrant a single gland was chosen, and systematic, nonoverlapping, random areas were examined in a Z shaped pattern; 4–6 photomicrographs were captured. Each gland was further split into four quadrants; two regions of interest (ROIs; 75 × 75 pixels) were randomly selected per quadrant and two measurements were taken from each quadrant with one measurement per ROI (eight measurements per gland, 32 measurements per slide). This method was validated by repeating the calculation the mean using different randomly selected measurements (always $n = 32$ measurements), with no significant differences in the mean values obtained. The mean values of the measurements were calculated for each case. All photomicrographs were taken at 100× magnification.

The EPC group was further analysed to assess the difference between inner and outer parts of the thickened capsule. As the BM of normal and DCIS was thin, such splitting into inner and outer was not possible and the whole BM was analysed as one part and the difference was considered between different ROIs. The inner part of the capsule was defined as the most adjacent part to tumour cells, while the outer capsule part was defined as the fibrous part adjacent to the stroma.

IMAGE ANALYSIS AND QUANTIFICATION OF COLLAGEN

Assessment of BM thickness and collagen distribution was undertaken using ImageJ (NIH, Bethesda, MD, USA, available for free download at <https://imagej.nih.gov/ij/download.html>).

Basement membrane thickness

Thickness of the BM and the EPC capsule was measured by calculating the average of 20 measurements for each case at 20× magnification.

Proportion of thin and thick fibres

The collagen fibres were distinguished as either thin or thick fibres using the polarised light, thin fibres were greenish yellow, and thick fibres appeared orange red.¹⁸ An ImageJ macro plugin recorder was used to automate channel separation for red, green, and background colours with quantification of the pixel area for each feature. Using the raw data output, the proportions and mean values of thin and thick collagen fibres were calculated for each case.

Collagen density

Assessment of collagen density was conducted via ImageJ split into RGB channels (red, blue, green); the blue and red images were then excluded. The green image was adjusted into a binary image with red foreground pixels designated as intensity 0 and the background was expressed as white pixels (intensity 255). All images were adjusted to a threshold of 150 to decrease noise. Integrated density was measured in pixels using the automated tools in ImageJ. The mean values for each case were calculated.

Collagen length, straightness, and width

Assessment of collagen fibre features using CT-FIRE (ctFIRE_V2.0Beta_WIN64_MCR2014b.exe) was conducted to extract individual fibres and to quantify the following measurements (units = pixels): mean fibre length—defined as the total contour of the fibres; mean fibre straightness—defined as the end-to-end length; and mean fibre width. The values for each of the fibres, from each image, for each tumour, were averaged to determine one value for each case.

Collagen fibre alignment and orientation

Assessment of collagen fibre features using Curve Align (CurveAlign_V4.0Beta_WIN64_MCR2014b.exe) was undertaken to extract individual fibres, and then quantify the following measurements: the alignment coefficients for each fibre, ranging from 0 to 1 for

each fibre, with 0 used to designate random alignment and 1 assigned as perfect alignment (alignment of fibres to each other); mean orientation angle (expressed as degrees ranging from 0 to 180°) that was calculated and defined as the alignment of each fibre to a horizontal line.

STATISTICAL ANALYSIS

For all statistical analysis, $P < 0.05$ was considered statistically significant and undertaken either in SPSSv26 (IBM, Armonk, NY, USA) or GraphPad Prism (Boston, MA, USA). Kruskal–Wallis, one-way analysis of variance (ANOVA), chi-square test, paired *T* test, and Wilcoxon signed ranks tests were used as specified in each result. Graphs and tables were constructed as applicable using GraphPad Prism. Results are expressed as the mean \pm SD of the mean throughout unless otherwise stated.

Results

CAPSULE AND BM THICKNESS AND COLLAGEN DISTRIBUTION

A significant increase in the thickness of the EPC capsule ($59.65 \pm 18.50 \mu\text{m}$) was found in comparison to the BMs in the normal breast tissue group ($0.032 \pm 0.009 \mu\text{m}$; $P < 0.0001$) and BMs from DCIS cases ($0.058 \pm 0.017 \mu\text{m}$; $P < 0.0001$) (Figure 1). In contrast, there was no difference between the BM thicknesses in the DCIS samples ($0.058 \pm 0.017 \mu\text{m}$) and normal breast tissue ($0.032 \pm 0.009 \mu\text{m}$; $P < 0.995$; Figure 1).

There was a significant increase in collagen density in the EPC capsules (53.47 ± 4.27 pixels) compared to both normal (18.43 ± 5.06 pixels) and DCIS (25.94 ± 8.02 pixels) BMs ($P < 0.0001$; Table 1, Figure 2).

Regarding the fibre types, most of the EPC capsule collagen was comprised of type I ($75.46 \pm 7.16\%$) compared to the BMs in both normal breast tissue ($25.25 \pm 12.27\%$) and DCIS ($29.86 \pm 6.81\%$; $P < 0.0001$). The EPC capsules showed a significant decrease in collagen III ($24.48 \pm 7.14\%$) compared to normal and DCIS BMs ($80.30 \pm 11.08\%$ and $68.86 \pm 7.88\%$, respectively, $P < 0.0001$) Table 1, Figures 2 and 3.

There was no statistically significant difference between BM of the normal breast tissue and those in DCIS regarding thickness ($P < 0.995$) or collagen distribution ($P < 0.07$). Contrary to this, there was

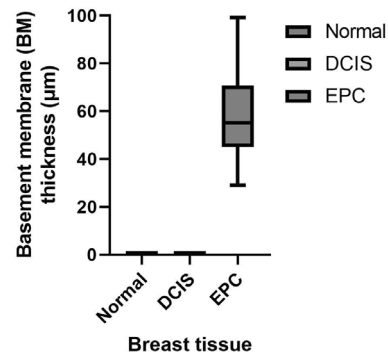


Figure 1. Thickness of the basement membrane in breast tissue. Measurements obtained on picrosirius PSR-stained histology specimens at 20 \times magnification, ImageJ, 20 measurements were obtained for each case. $N = 25$ cases/group. Normal: Normal breast tissue; DCIS, Ductal carcinoma *in situ*; EPC, Encapsulated papillary carcinoma capsule, one-way ANOVA with post-hoc test, $F = 232.07$, $P < 0.0001$.

a significant increase of collagen density in DCIS cases ($P < 0.0001$).

COLLAGEN FIBRE CHARACTERISTICS

The EPC capsules showed significant increases in fibre width (7.78 ± 0.15 pixels, $P < 0.0001$) and decreases in length (56.53 ± 2.74 pixels, $P < 0.0001$) compared to both normal and DCIS BM width (7.05 ± 0.15 and 7.07 ± 0.2 pixels, respectively) and length (61.66 ± 2.78 and 61.61 ± 3.89 pixels, respectively). EPC capsules also had straighter fibres (0.95 ± 0.004 on a 0–1 scale) compared to BMs in both normal breast tissue (0.92 ± 0.007 on a 0–1 scale) and DCIS (0.93 ± 0.005 on a 0–1 scale, $P < 0.0001$). No significant differences were observed between normal and DCIS BMs in either fibre width ($P < 0.96$) or length ($P < 1$); however, DCIS BM fibres were considered more straight in formation compared to those in normal BMs ($P < 0.0001$; Table 1, Figure 4).

DIRECTIONALITY OF COLLAGEN FIBRES

EPC capsule fibres presented with less alignment (0.34 ± 0.07 on a 0–1 scale) compared to normal and DCIS BMs (0.57 ± 0.08 and 0.40 ± 0.09 , respectively, on a 0–1 scale, $P < 0.0001$, Table 1, Figure 4). There was also a decrease in fibre alignment in the DCIS BM compared to normal BMs ($P < 0.0001$; Table 1, Figure 5).

The orientation angles of the collagen fibres were classified as either ‘parallel’ or ‘perpendicular’ for each

case observed based on the dominant angle measurement. Angles of 70–110° were considered 'perpendicular' fibres and measurements outside of this were considered 'parallel'. Comparisons were made between the numbers of cases in each group classified as having

either 'parallel' or 'perpendicular' fibres in the BM. Most of the cases within the EPC group showed more 'perpendicular' fibre (96%) compared to DCIS (60%), whereas no cases in the normal tissue had perpendicular fibres in their BMs. Conversely, 4% of EPC cases had

Table 1. Characteristics of collagen fibres within EPC capsules in breast tissue

Parameter	Group	The mean	Standard error of mean (SEM)	Tissue comparisons	P value
Mean fibre density (pixels)	Normal	18.43	1.013	DCIS	0.0001*
				EPC	0.0001*
				Invasive	0.0001*
	DCIS	25.94	1.604	EPC	0.0001*
				Invasive	0.0001*
	EPC	53.46	0.854	Invasive	0.0001*
	Invasive	38.90	1.292	—	—
	Collagen III fibre content (%)	Normal	80.30	2.217	DCIS
EPC					0.0001*
Invasive					0.0001*
DCIS		68.86	1.557	EPC	0.0001*
				Invasive	0.0001*
EPC		24.48	1.427	Invasive	0.367
Invasive		28.08	1.410	—	—
Collagen I fibre content (%)		Normal	25.25	2.454	DCIS
	EPC				0.0001*
	Invasive				0.0001*
	DCIS	29.86	1.362	EPC	0.0001*
				Invasive	0.0001*
	EPC	75.46	1.431	Invasive	0.388
				Invasive	71.92
	Mean fibre width (pixels)	Normal	7.074	0.030	DCIS
EPC					0.0001*
Invasive					0.0001*
DCIS		7.075	0.039	EPC	0.0001*
				Invasive	0.0001*
EPC		7.777	0.031	Invasive	0.980
Invasive		7.755	0.054	—	—

Table 1. (Continued)

Parameter	Group	The mean	Standard error of mean (SEM)	Tissue comparisons	P value
Mean fibre length (pixels)	Normal	61.66	0.557	DCIS	1
				EPC	0.0001*
				Invasive	0.0001*
	DCIS	61.61	0.779	EPC	0.0001*
				Invasive	0.0001*
	EPC	56.53	0.549	Invasive	0.0001*
	Invasive	51.22	0.677	—	—
	Mean fibre straightness scale (0–1)	Normal	0.922	0.001	DCIS
EPC					0.0001*
Invasive					0.0001*
DCIS		0.934	0.001	EPC	0.0001*
				Invasive	0.0001*
EPC		0.953	0.001	Invasive	0.0001*
Invasive		0.943	0.001	—	—
Mean Alignment coefficient scale (0–1)		Normal	0.569	0.015	DCIS
	EPC				0.0001*
	Invasive				0.0001*
	DCIS	0.397	0.017	EPC	0.039*
				Invasive	0.0001*
	EPC	0.342	0.014	Invasive	0.0001*
	Invasive	0.184	0.006	—	—

Normal, Normal breast tissue; DCIS, Ductal carcinoma *in situ*; EPC, Encapsulated papillary carcinoma capsule; Invasive, Invasive breast carcinoma.

* $P < 0.05$.

'parallel' fibres compared to 40% of DCIS cases. All cases of normal breast tissue group had 'parallel' fibres ($P < 0.0001$, Table 2, Figure 5).

COMPARISON BETWEEN EPC CAPSULE AND BM-LIKE MATERIAL IN INVASIVE TUMOURS

There was a significant increase in collagen fibre density in EPC capsule cases (53.47 ± 4.27 pixels) compared to the invasive group BM-like material (38.90 ± 6.46 pixels, $P < 0.0001$), with no difference in collagen fibre content for either collagen I ($P < 0.86$) or collagen III ($P < 0.37$). In addition, EPC capsule fibres showed a significant increase in length and straightness (both $P < 0.0001$) compared

to invasive fibres, while there were no significant differences in fibre width between both groups ($P < 0.98$). With regard to collagen fibre directions, EPC cases showed more aligned fibres compared to the invasive group ($P < 0.0001$; Table 1).

COMPARISON BETWEEN EPC CAPSULE AND ENCAPSULATED PAPILLARY THYROID CARCINOMA (EPTC) CAPSULE

There was no significant difference between the EPC and EPTC capsule thickness (59.65 ± 18.50 and 57.76 ± 13.86 μm , respectively, $P = 0.77$; Figure 6) or fibre density (53.47 ± 4.27 and 55.29 ± 3.74 pixels, respectively, $P = 0.25$).

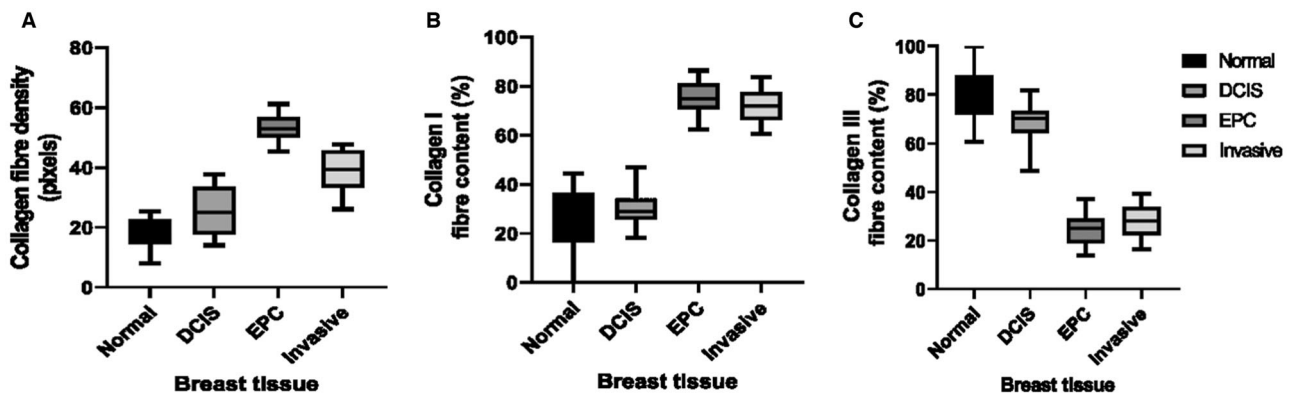


Figure 2. Collagen distribution within breast tissue basement membrane (BM). (A) Collagen fibre density, one-way ANOVA with post-hoc test, $F = 157.81$, $P < 0.0001$. (B) Percentage of collagen type I fibre content, Kruskal–Wallis test, $H = 75.62$, $P < 0.0001$. (C) Percentage of collagen type III fibre content Kruskal–Wallis test, $H = 78.25$, $P < 0.0001$. Measurements obtained on picrosirius (PSR)-stained histology specimens at $100\times$ magnification, ImageJ, 32 measurements were obtained for each case. $N = 25$ cases/group. Normal: Normal breast tissue; DCIS, Ductal carcinoma *in situ*; EPC, Encapsulated papillary carcinoma capsule; Invasive, Invasive breast carcinoma.

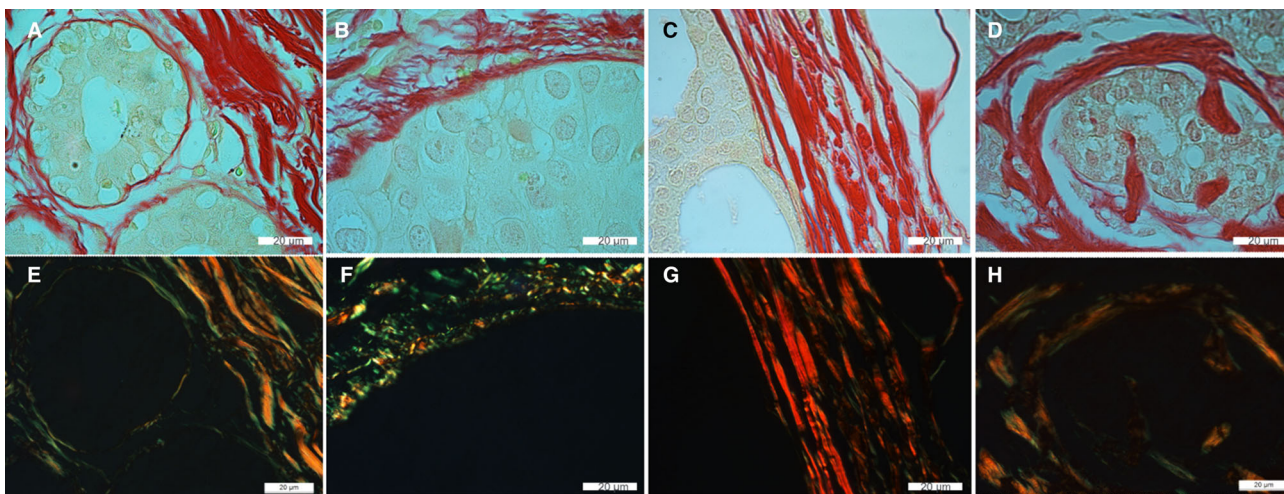


Figure 3. Photomicrographs of basement membrane (BM) within breast tissue. (A) Normal breast tissue stained with picrosirius red (PSR) depicting a normal gland lined with simple cubical epithelium surrounded by well-defined BM. (B) Ductal carcinoma *in situ* (DCIS) stained with PSR depicting part of a breast gland undergoing cell proliferation surrounded by a definite BM. (C) Encapsulated papillary carcinoma (EPC) stained with PSR depicting part of the capsule. (D) Invasive carcinoma tissue type adenoid cystic carcinoma stained with PSR showing neoplastic cells surrounded by BM-like material. (E) Normal breast tissue stained with PSR and examined under polarised light (PL) indicating greenish collagen fibres in the BM surrounding the gland (shown in black). (F) DCIS tissue stained with PSR and examined under PL showing BM with green collagen fibres surrounded by the gland (shown in black). (G) EPC stained with PSR and examined under PL showing with collagen expressed as orange to red fibres. (H) Invasive carcinoma tissue type adenoid cystic carcinoma stained with PSR and examined under PL showing BM-like material with a range of green to yellow/orange collagen fibres. Magnification $\times 100$, scale bar depicts $20\ \mu\text{m}$.

Regarding the fibre types, most of the collagen within both the EPC and EPTC capsules was collagen I ($75.46 \pm 7.16\%$ versus $76.43 \pm 10.31\%$, respectively; $P < 0.36$) and collagen III ($24.48 \pm 7.14\%$ versus $19.89 \pm 6.08\%$, respectively; $P < 0.05$; Figures 7 and 8). There were also no significant differences between EPC capsule fibre width (7.78 ± 0.15 pixels) and length (56.53 ± 2.74 pixels) compared to EPTC

capsule fibre width (7.61 ± 0.35 pixels; $P = 0.06$) and length (54.85 ± 3.59 pixels $P = 0.14$).

In contrast, the EPC capsules did present with straighter fibres (0.95 ± 0.004 on a 0–1 scale) compared to those within the EPTC capsule (0.94 ± 0.005 on a 0–1 scale; $P < 0.034$). In terms of directionality, the EPC capsule fibres presented with less alignment (0.34 ± 0.07 on a 0–1 scale) compared to those in the

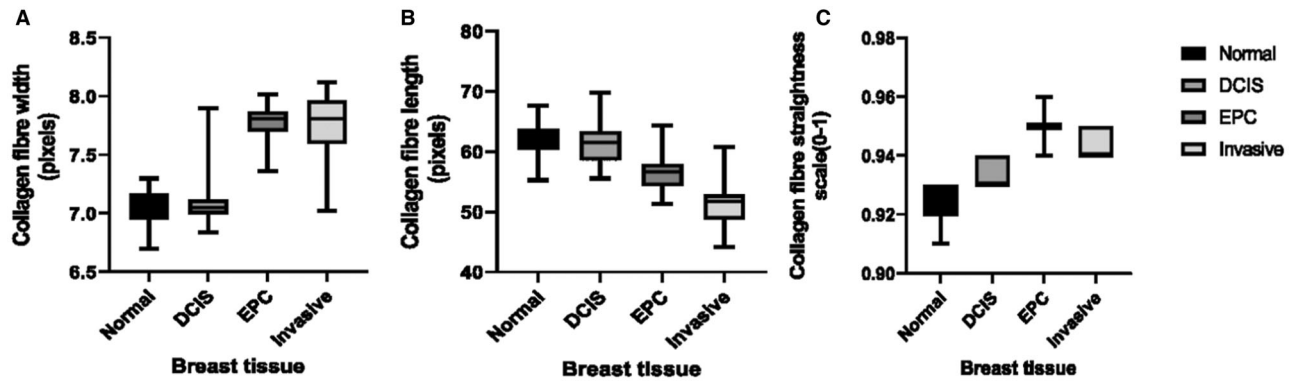


Figure 4. Collagen fibre characteristics within breast tissue basement membrane (BM). (A) Collagen fibre width, $F = 101.94$, $P < 0.0001$. (B) Collagen fibre length, $F = 59.07$, $P < 0.0001$. (C) Collagen fibre straightness, $F = 123.34$, $P < 0.0001$. Measurements obtained on picrosirius (PSR)-stained histology specimens at $100\times$ magnification, CT-Fire, 32 measurements were obtained for each case. $N = 25$ cases/group. Normal: Normal breast tissue; DCIS, Ductal carcinoma *in situ*; EPC, Encapsulated papillary carcinoma capsule; Invasive, Invasive breast carcinoma. One-way ANOVA with post-hoc test.

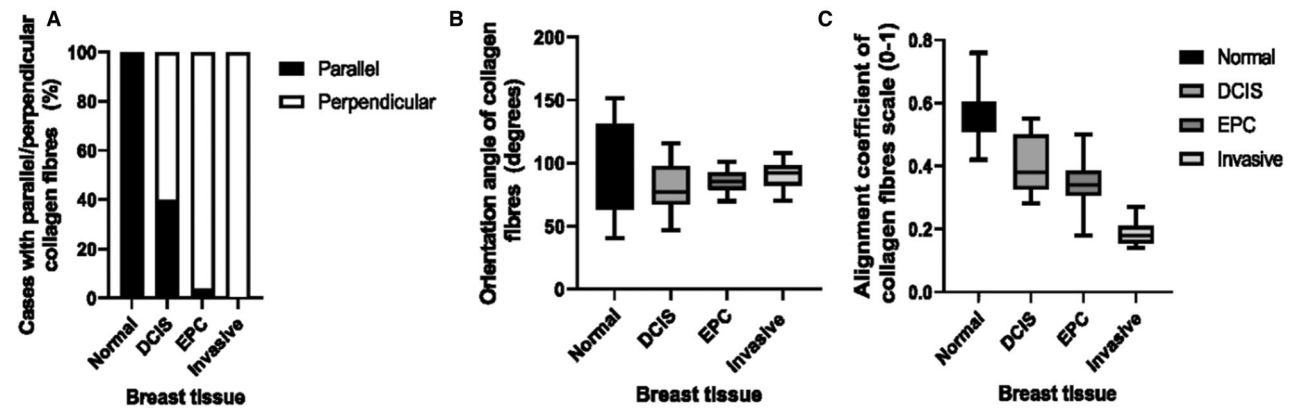


Figure 5. Collagen fibre directionality within breast tissue basement membrane (BM). (A) The percentages of cases with parallel ($<70^\circ$ or $>110^\circ$) or perpendicular fibres ($\geq 70^\circ - \leq 110^\circ$). (B) Collagen fibre orientation angle, Chi-square; $\chi^2 = 69.79$, $P < 0.0001$. (C) The coefficient alignment of collagen fibres, one-way ANOVA with post-hoc test $F = 122.05$, $P 0.0001$. Measurements were obtained on picrosirius (PSR)-stained histology specimens at $100\times$ magnification. Curve-align, 32 measurements were obtained for each case. $N = 25$ cases/group. Normal: Normal breast tissue; DCIS, Ductal carcinoma *in situ*; EPC, Encapsulated papillary carcinoma capsule; Invasive, Invasive breast carcinoma.

Table 2. Collagen fibre orientation angles within breast tissue basement membranes

Group	Mean orientation angle	Standard deviation (SD)	Parallel fibres (%)	Perpendicular fibres (%)
Normal	102.8	32.20	100	0
DCIS	80.58	19.48	40	60
EPC	86.28	8.48	4	96
Invasive	90.79	9.42	0	100

EPTC capsules (0.38 ± 0.04 on a 0–1 scale); however, the difference was not significant ($P = 0.12$). 96% of EPC (96%) had ‘perpendicular’ fibre compared to 80% of EPTC but the difference was not significant (Figure 8).

HETEROGENEITY OF THE EPC CAPSULE

Comparisons of measurements between the inner and outer parts of the capsule tissue were also undertaken in the EPC group. This showed that the outer part of the capsule had significantly higher collagen density (42.50 ± 1.78 pixels; paired *t*-test, $t = 5.88$,

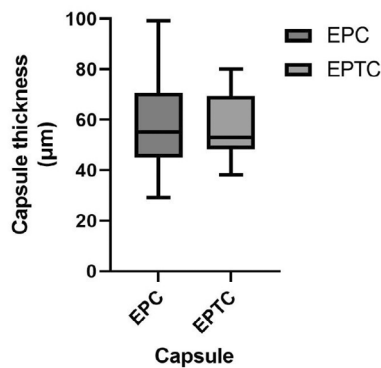


Figure 6. Capsule thickness. Measurements were obtained on picrosirius PSR-stained histology specimens at 20× magnification, ImageJ. 20 measurements were obtained for each case. EPC, encapsulated papillary carcinoma capsule; EPTC, Encapsulated papillary thyroid carcinoma. Independent *t* test $t = 0.881$, $P < 0.77$.

$P < 0.0001$) with more collagen I ($75.46 \pm 7.16\%$; $Z = -4.238$, $P < 0.0001$) compared to the inner part density and collagen I (40.47 ± 1.31 pixels; $59.31 \pm 13.79\%$, respectively). Conversely, the inner capsule had more collagen III ($40.69 \pm 13.79\%$; $Z = -4.238$, $P < 0.0001$) compared to the outer part ($24.54 \pm 7.16\%$; Figures 9 and 10).

There was a statistically significant increase in mean fibre width in the outer part of the capsule (7.78 ± 0.015 pixels) compared to the inner part of the capsule (7.36 ± 0.094 pixels; paired *t* test, $t = -11.90$, $P < 0.0001$). There were no significant differences in mean fibre lengths within both the inner and outer capsule (57.59 ± 1.62 compared to 57.05 ± 1.99 pixels, respectively; $t = -1.35$, $P < 0.19$). The outer capsule fibres showed more straightness (0.95 ± 0.005 on a scale of 0–1) compared to the inner part (0.94 ± 0.007 ; Wilcoxon signed ranks test, $Z = -4.32$, $P < 0.0001$). Capsular collagen fibres of the outer part were also less aligned than the inner part ($t = -6.07$, $P < 0.0001$; Figure 10).

COMPARISON BETWEEN EPC CAPSULAR HETEROGENEITY AND OTHER GROUPS

Both EPC capsular parts inner (40.47 ± 1.31 pixels) and outer (42.50 ± 1.78 pixels) showed increased collagen density ($P < 0.0001$) compared to other groups (normal, DCIS, and invasive), and showed higher collagen I content and lower collagen III compared to other groups except the invasive group (Table 3). In contrast, there was no significant difference in both collagen I and III (both $P < 0.38$)

content between the outer part of the capsule and invasive groups. Both the inner and outer parts showed increases in fibre width, length, and straightness compared to other groups (all $P < 0.0001$), while the outer part showed no significant difference in width compared to the invasive group ($P < 0.97$) and the inner part showed no significant difference regarding alignment ($P < 1$) compared to the invasive group, or straightness with both DCIS and invasive ($P < 0.13$ and $P < 0.94$, respectively). These results are shown in Table 3 and Figure 11.

Discussion

PC remains a controversial entity regarding morphological features, histological categorization, and clinical management. Although the biological behaviour of papillary DCIS and invasive PC is well established, the categorization of EPC into *in situ* or invasive disease remains challenging and problematic, resulting in management implications as categorizing as an invasive lesion may trigger adjuvant systematic therapy.¹⁹

The current study results showed that the BM that surround the normal ducts and lobules in normal breast tissue had predominantly collagen type III fibres, with thinner, shorter, and more curved fibres, which were parallel to the duct border and showed good alignment to each other. The DCIS BMs were similar to normal breast tissue but exhibited higher density and less aligned straighter fibres. However, the BM-like material that surrounded the invasive group tissue showed a high density of collagen fibres with increased proportions of collagen I and decreased collagen III, with thicker, shorter, straighter, and less aligned fibres.

A study of EPC showed that the presence of collagen IV and laminin in all cases of pure EPCs with an absence of their expression in a significant percentage of EPCs associated with invasive breast cancer, and these results were used to indicate that these collagen IV and laminin-positive tumours may be characterised as *in situ* lesions.¹ However, laminin and collagen IV can be seen in the wound-healing process, and therefore not specific for the native BM characteristic of *in-situ* tumours.^{20,21} Moreover, a similar peripheral capsule-like structure can be seen surrounding invasive tumour foci in other tissues outside the breast, supporting the theory that this is a reactive process rather than BM expansion.⁴ In addition, some cases of typical EPC with a well-developed capsule have been reported with local muscle infiltration,²² lymph node metastasis,^{22–24} or distant

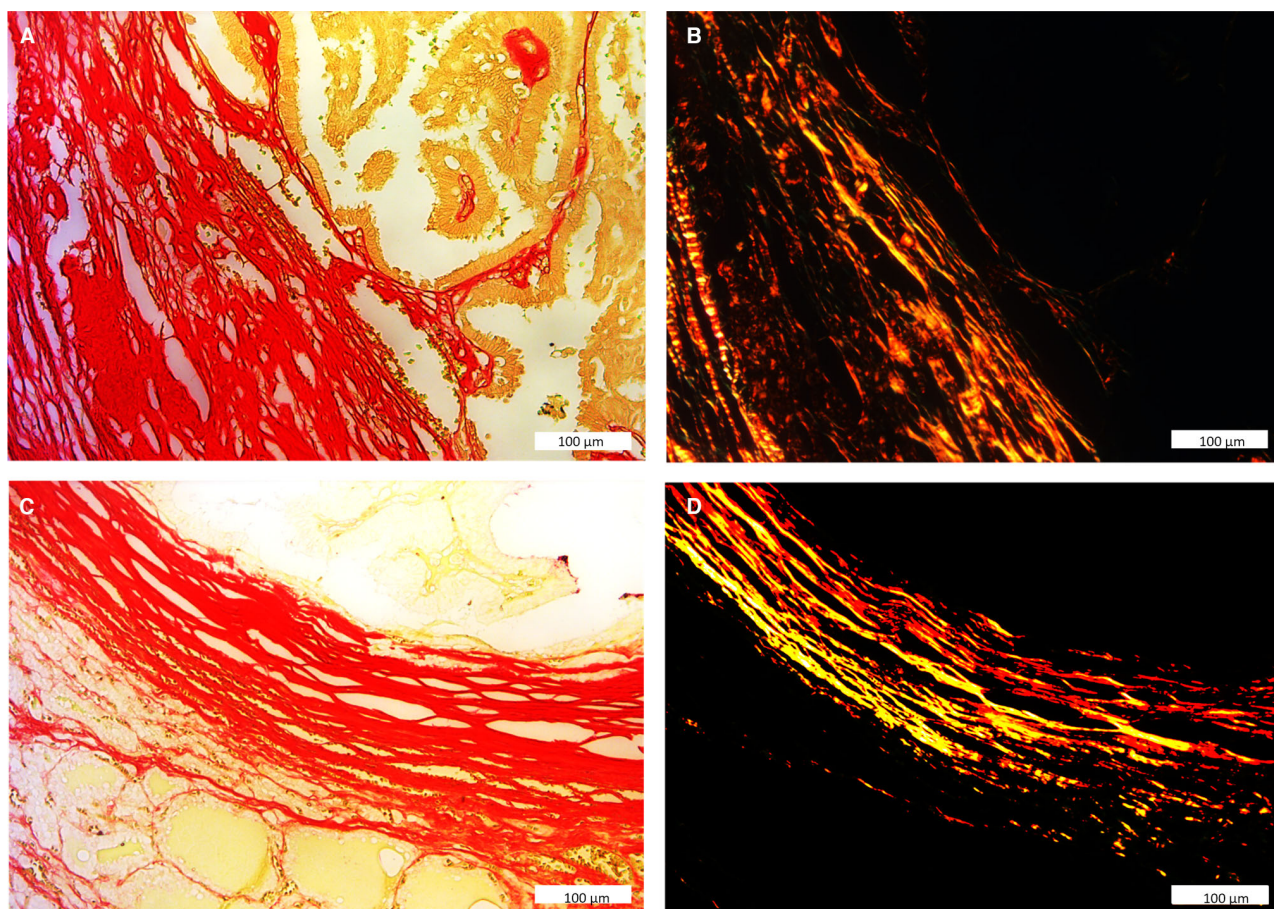


Figure 7. Photomicrographs of capsules within various cancer tissues. (A) Encapsulated papillary carcinoma (EPC) stained with PSR depicting part of the capsule. (B) EPC stained with PSR and examined under polarised light showing collagen expressed as orange to red fibres. (C) Encapsulated papillary thyroid carcinoma (EPTC) stained with PSR depicting part of the capsule and thyroid follicles. (D) EPTC stained with PSR and examined under polarised light showing collagen expressed as orange to red fibres.

metastases^{25–27} and a similar capsule-like structure is seen around some of the EPC foci at the distant sites.²² These findings argue against the surrounding capsule of EPC that lack MEC being a native but thickened BM characteristic of the intraductal lesions and provides further evidence that these lesions are invasive carcinomas with an indolent behaviour and expansile growth pattern.³

Not all sheet like structures at the epithelial stroma interface represent BM. A true capsule is defined as a rim of relatively pure fibrous tissue (composed predominantly of collagen) around a tumour, while a pseudocapsule is defined as mixed fibrous tissue and entrapped normal structures around the tumour. A pseudocapsule is mainly caused by the expansive growth of the tumour and a combination of the mechanical effect of the compression of the surrounding tissue and condensation of scarring that occurs as

a body defence mechanism against tumours. Meanwhile, a true capsule is a biological process resembling wound-healing responses and has morphological integrity. Many tumours, including benign and malignant, *in situ*, and invasive, exhibit an encapsulation process; however, the distinction between true and pseudocapsules varies based on the context.⁶

The present study compared the characteristics of collagen fibres in EPC capsules with the BMs of normal and DCIS, as well as with the BM-like material that is present in some invasive breast tumours. This showed that EPCs had a thickened capsule with denser collagen fibres, enriched with stromal-type collagen (collagen I) with thicker, shorter, straighter, and more disorganised fibres than that of the BM of DCIS or normal breast tissue. The present study also demonstrated that the EPC capsule exhibited no significant difference to the BM-like material

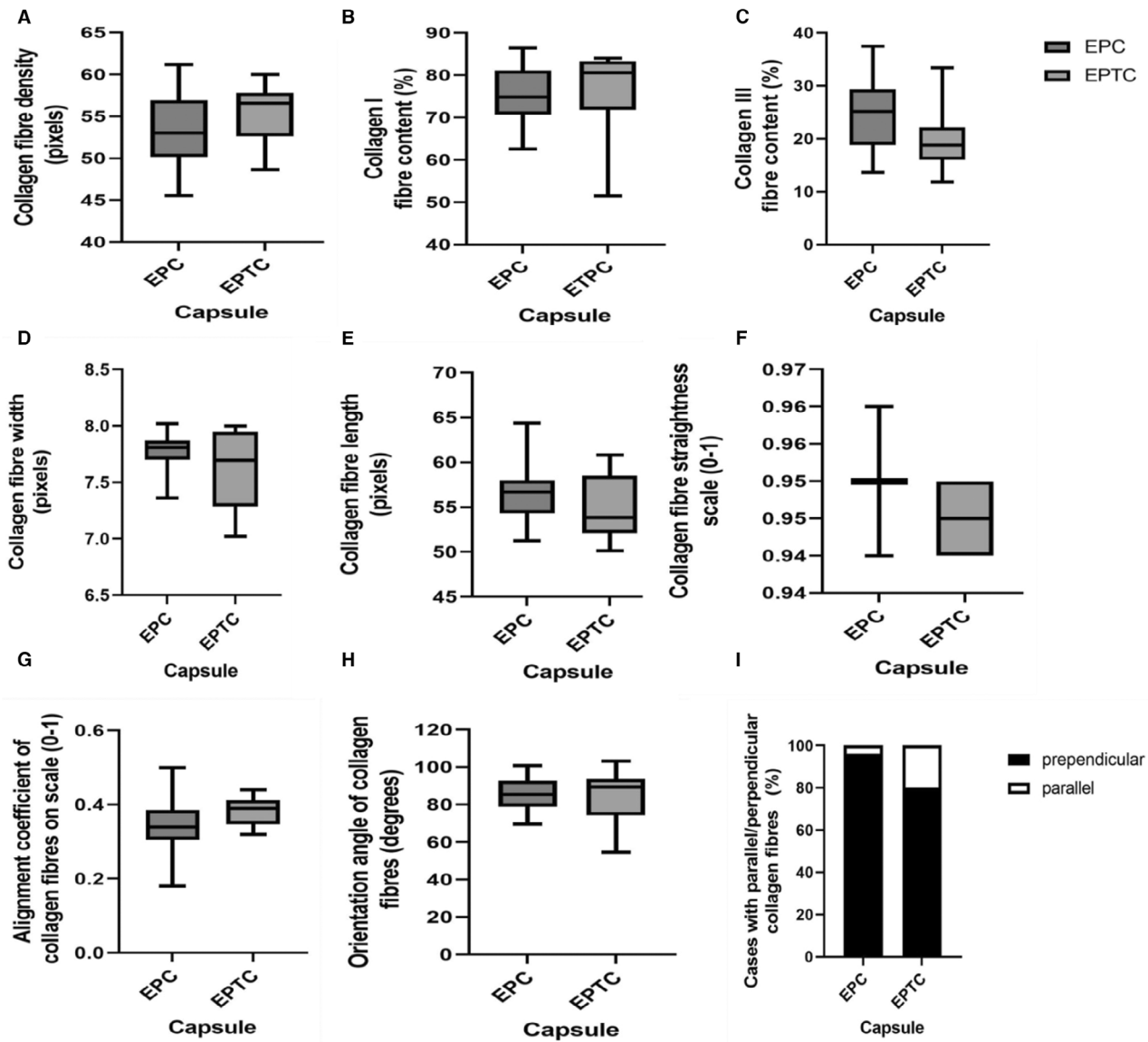


Figure 8. Comparison between encapsulated papillary carcinoma (EPC) and encapsulated papillary thyroid carcinoma (EPTC). (A) Collagen fibre density, Independent *t* test, $t = 0.27$, $P < 0.24$. (B) Collagen I fibre content, Mann–Whitney *U* test, $U = 151$, $P < 0.35$. (C) Collagen III fibre content, $U = 74$, $P < 0.06$. (D) Collagen fibre width Independent *t* test, $t = 10.46$, $P < 0.06$. (E) Collagen fibre length Independent *t* test, $t = 1.69$, $P < 0.14$. (F) Collagen fibre straightness, Mann–Whitney *U* test, $U = 67.5$, $P < 0.034$. (G) The coefficient alignment of collagen fibres Independent *t* test, $t = 2.4$, $P < 0.16$. (H) Collagen fibre orientation angle. (I) The percentages of cases with parallel ($<70^\circ$ or $>110^\circ$) or perpendicular fibres ($\geq 70^\circ$ – $\leq 110^\circ$), Chi-square; $\chi^2 = 0.41$; $P < 1$. Measurements were obtained on picrosirius (PSR)-stained histology specimens at 100 \times magnification; 32 measurements were obtained for each case using ImageJ, CT-FIRE, and Curve align.

surrounding the invasive types regarding many characteristics such as collagen I and collagen III fibre content, and fibre width. In addition, EPC capsules showed marked heterogeneity between their inner and outer parts, with the inner part resembling the DCIS BM only in fibre straightness; however, there was a significant increase in the capsule thickness.

The outer part of EPC capsules exhibited no significant differences relating to fibre density, width, or collagen distribution (I and III) compared to the invasive tissue.

A previous study showed that EPC lesions express higher levels of TGF β 1 compared with DCIS and invasive carcinomas, which plays a role in the

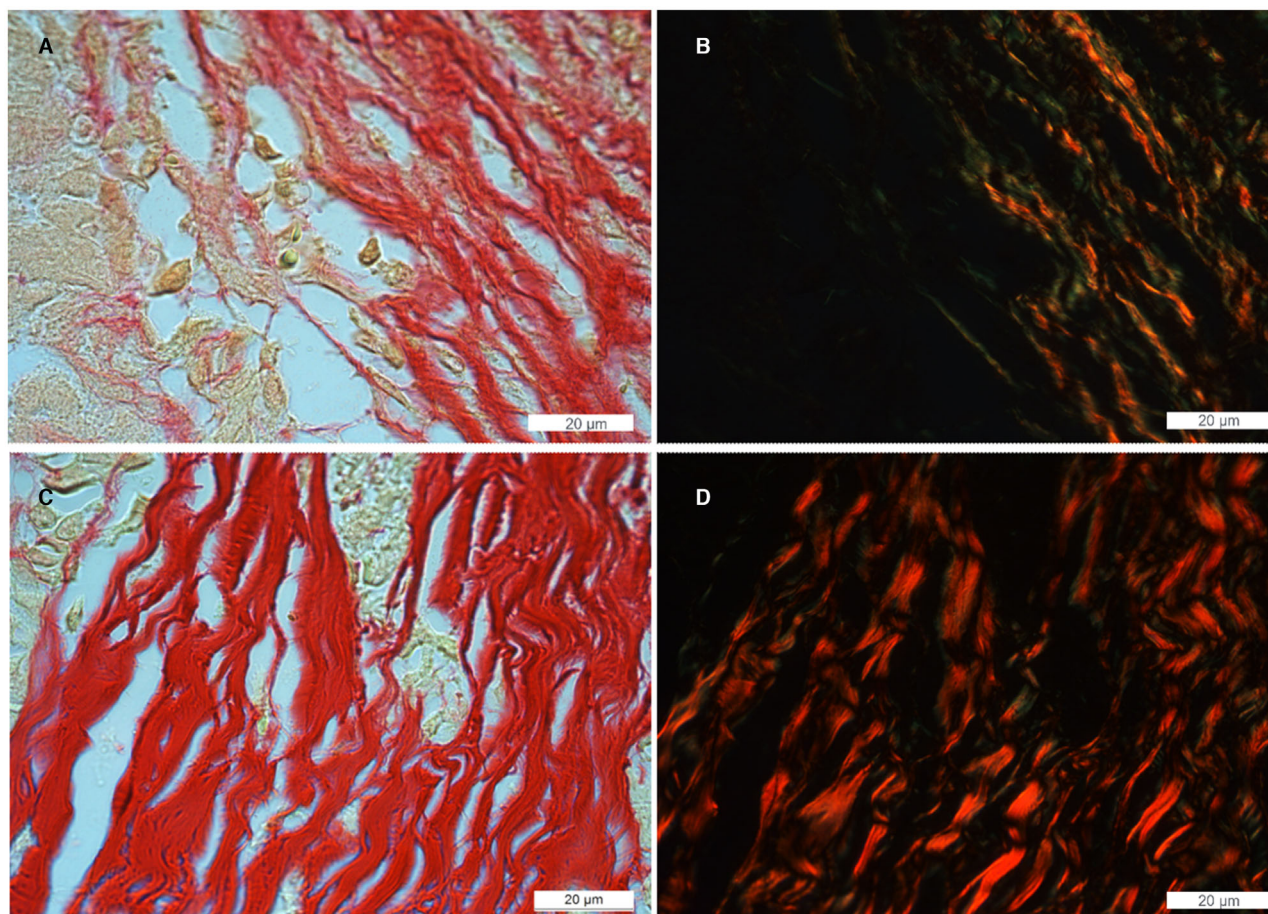


Figure 9. Encapsulated papillary carcinoma (EPC) capsular heterogeneity. (A) Inner part of EPC stained with picrosirius red (PSR) stain showing collagen fibres. (B) Inner part of EPC stained with PSR and examined under polarised light (PL) showing part of the capsule with straight collagen fibres ranging in colour from green to orange. (C) Outer part of EPC capsule stained with PSR showing wavy collagen fibres. (D) Outer part of EPC capsule stained with PSR and examined under PL showing collagen expressed as orange to red wavy fibres. Magnification $\times 100$, Scale bars depict 20 μm .

development of the thick fibrous capsule, supporting the hypothesis that the EPC capsule is a reactive rather than a thickened expanded native BM resulting from distention by the proliferation of neoplastic papillary.³ These observations were consistent with the results from the present study. All of the DCIS, EPC capsule (inner and outer), and invasive group cases had fewer thin fibres compared to the control group. In addition, this study showed that most of the EPC capsule collagen was type I compared to BMs from both normal breast tissue and DCIS, with no difference exhibited when compared with the BM-like material in invasive tumours.

Many previous studies focused on the distribution of collagen IV around EPC to examine whether this tumour was *in situ* or invasive. Esposito *et al.* concluded that most cases of EPC were surrounded by

collagen IV.⁹ Wynveen *et al.* identified continuous, high intense layers (3+ positivity) of collagen IV in three cases; however, most cases had discontinuous and fragmented (1+, 2+) expression and only one case exhibited no collagen IV reactivity.²⁸ Golestani *et al.* demonstrated the presence of continuous, uniform, and strong collagen IV immunostaining around all EPC cases.²⁹ In addition, Akladois *et al.* documented the presence of BM around EPC by positive collagen IV staining.³⁰ However, the presence of BM components surrounding EPCs cannot be considered as evidence for *in situ* carcinomas, as this finding has been detected in a subset of invasive breast cancers and in nodal metastases.^{31–33}

Encapsulated papillary thyroid carcinoma (EPTC), which is an indolent carcinoma with rare recurrence or lymph nodal metastases^{34–38} exhibits excellent

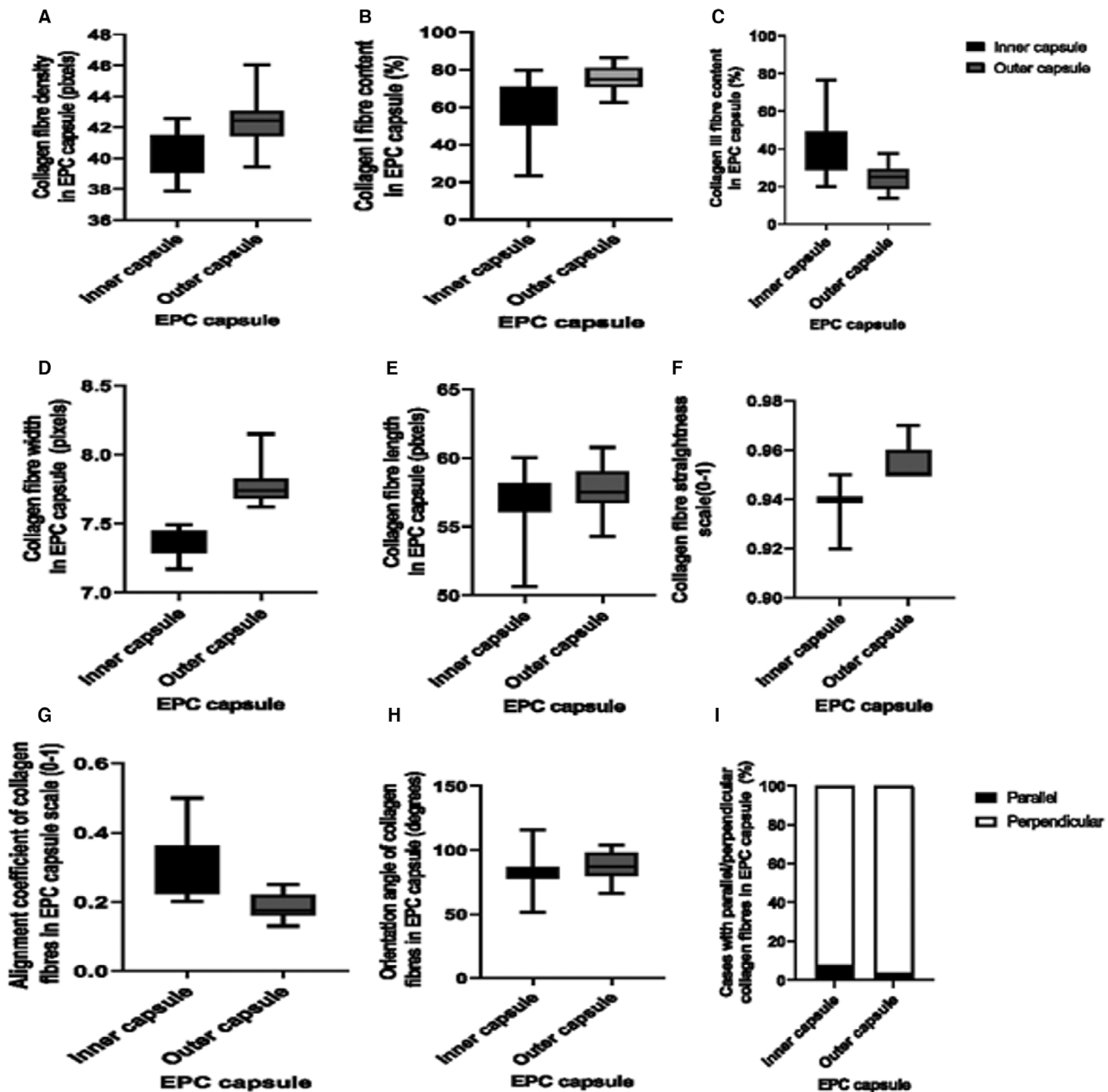


Figure 10. Encapsulated papillary carcinoma (EPC) capsular heterogeneity. (A) Collagen fibre density paired t test, $t = 5.88$, $P < 0.0001$. (B) Collagen I fibre content, Wilcoxon signed ranks test, $Z = -4.238$, $P < 0.0001$. (C) Collagen III fibre content, $Z = -4.238$, $P < 0.0001$. (D) Collagen fibre width paired t test, $t = -11.90$, $P < 0.0001$. (E) Collagen fibre length paired t test, $t = -1.35$, $P < 0.19$. (F) Collagen fibre straightness, Wilcoxon signed ranks test, $Z = -4.32$, $P < 0.0001$. (G) The coefficient alignment of collagen fibres paired t test, $t = 6.14$, $P < 0.0001$. (H) Collagen fibre orientation angle. (I) The percentages of cases with parallel ($<70^\circ$ or $>110^\circ$) or perpendicular fibres ($\geq 70^\circ \leq 110^\circ$), Chi-square; $\chi^2 = 0.355$; $P < 0.55$. Measurements were obtained on picrosirius (PSR)-stained histology specimens at $100\times$ magnification; 32 measurements were obtained for each case using ImageJ, CT-FIRE, and Curve align.

prognosis,^{39,40} it is also typically surrounded by a fibrous tissue capsule similar to EPC. Quantitative analysis of collagen fibres using Second Harmonic Generation (SHG) microscopy revealed that EPTC

capsules had more dispersed collagen fibres than benign tumour capsules. In line with our findings, Bayadsi *et al.*,⁴¹ reported that EPTC had higher amounts of collagen I within the capsule using

Table 3. Characteristics of capsule heterogeneity in EPC

Parameter	Group	The mean	Standard error of mean (SEM)	Tissue comparisons	P value			
Mean fibre density (pixels)	Normal	18.43	1.013	DCIS	0.0001*			
				In EPC	0.0001*			
				Out EPC	0.0001*			
				Invasive	0.0001*			
	DCIS	25.94	1.604	In EPC	0.0001*			
				Out EPC	0.0001*			
				Invasive	0.0001*			
				In EPC	40.47	1.48	Out EPC	0.644
	Invasive	0.827						
	Out EPC	42.50	1.48				Invasive	0.113
							Invasive	38.90
	Collagen III fibre content (%)	Normal	80.30	2.217	DCIS	0.128		
In EPC					0.0001*			
Out EPC					0.0001*			
Invasive					0.0001*			
DCIS		68.86	1.557	In EPC	0.001*			
				Out EPC	0.0001*			
				Invasive	0.0001*			
				In EPC	38.69	2.759	Out EPC	0.002*
Invasive		0.032*						
Out EPC		9.97	1.431				Invasive	0.381
							Invasive	28.08
Collagen I fibre content (%)		Normal	25.25	2.454	DCIS	0.514		
	In EPC				0.0001*			
	Out EPC				0.0001*			
	Invasive				0.0001*			
	DCIS	29.86	1.362	In EPC	0.0001*			
				Out EPC	0.0001*			
				Invasive	0.0001*			
				In EPC	61.21	2.759	Out EPC	0.002*
	Invasive	0.30*						
	Out EPC	90.07	1.431				Invasive	0.381
							Invasive	71.92

* $P < 0.05$.

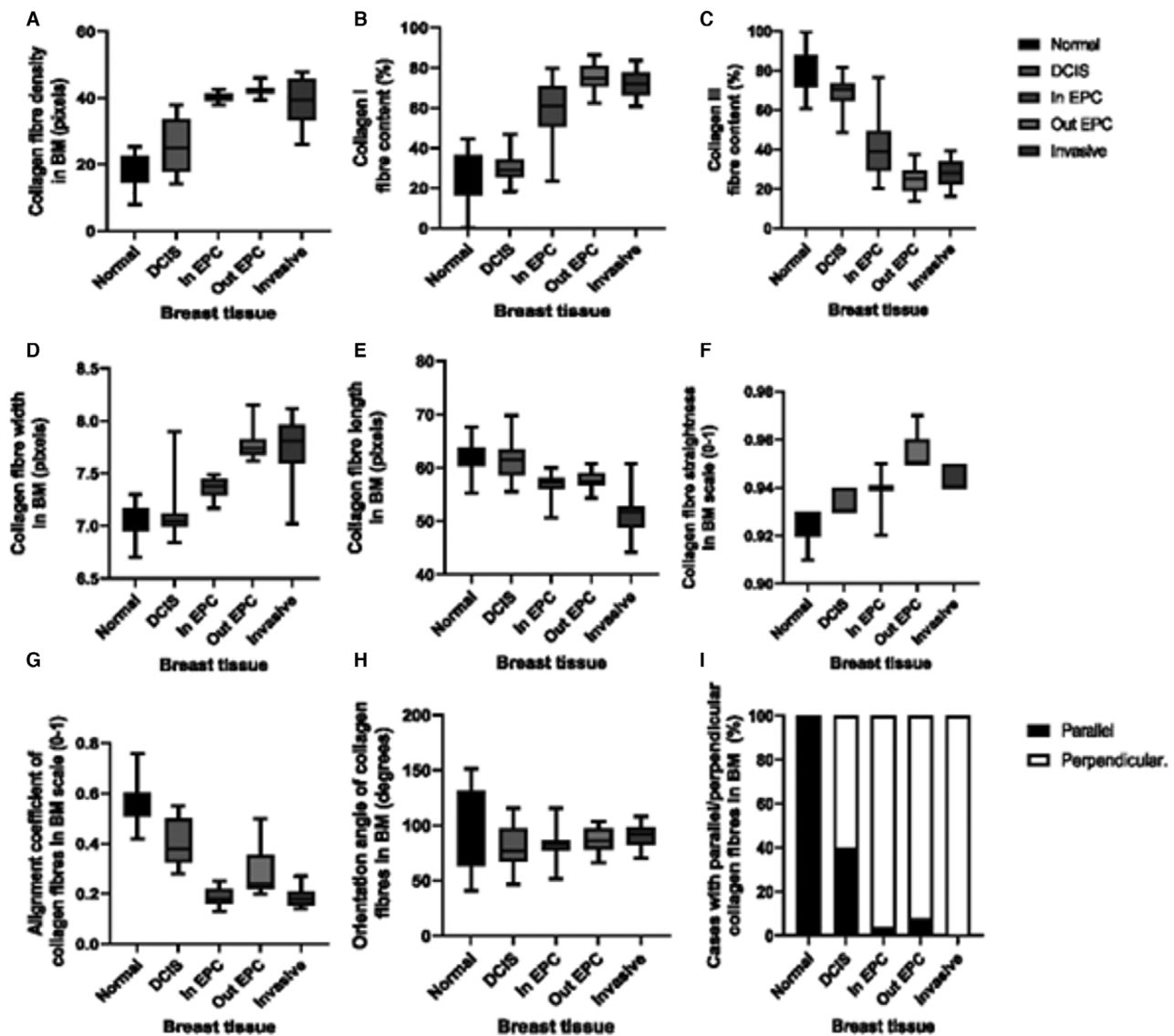


Figure 11. Comparison of encapsulated papillary carcinoma (EPC) heterogeneity with breast tissue basement membranes. (A) Collagen fibre density, one-way ANOVA with post-hoc test, $F = 61.05$, $P < 0.0001$. (B) Collagen I fibre content, Kruskal–Wallis test, $H = 94.655$, $P < 0.0001$. (C) Collagen type III fibre content, Kruskal–Wallis test, $H = 96.876$, $P < 0.0001$. (D) Collagen fibres width, one-way ANOVA test, $F = 93.111$, $P < 0.0001$. (E) Collagen fibres length, one-way ANOVA test, $F = 55.851$, $P < 0.0001$. (F) Collagen fibre straightness, one-way ANOVA test, $F = 87.342$, $P < 0.0001$. (G) The coefficient alignment of collagen fibres, one-way ANOVA test, $F = 136.592$, $P < 0.0001$. (H) Collagen fibre orientation angle. (I) The percentages of cases with parallel ($<70^\circ$ or $>110^\circ$) or perpendicular fibres ($\geq 70^\circ$ – $\leq 110^\circ$), Chi-square: $\chi^2 = 83.409$, $P < 0.0001$. Measurements were obtained on picrosirius (PSR)-stained histology specimens at $100\times$ magnification; 32 measurements were obtained for each case using ImageJ, CT-FIRE, and Curve align. $N = 25$ cases/group.

immunohistochemistry. Additionally, other invasive tumours with indolent behaviour characterised by pushing borders and surrounded by a fibrous capsule that contained both collagen IV and collagen I fibres, including hepatocellular carcinoma^{42–46} and some forms of prostate adenocarcinoma.⁴⁷ This was consistent with results obtained in the present study.

Renal papillary carcinoma is an encapsulated tumour in the kidney⁴⁸ that is surrounded by a fibromuscular capsule that has a complex of collagen fibres and smooth muscle.⁴⁹ Many studies have detected collagen IV in the renal pseudocapsule.^{50–52} However, Lohi *et al.*, in their study of collagen type IV $\alpha 1(IV)$ – $\alpha 6(IV)$ expression in renal carcinoma showed that papillary the

carcinoma capsule had only collagen IV alpha 5 chain.⁵³ Another study that characterised papillary carcinoma capsule using multiphoton microscopy showed that there was a significant difference in thickness and collagen area variation within each tumour; however, the thickest and thinnest parts showed no significant differences regarding collagen density or fibre directions.⁵⁴ In addition, when comparing papillary renal carcinoma with other types, it showed a lower rate of capsule completeness and presence.⁵⁴ Stamatou *et al.* demonstrated that a renal carcinoma capsule expressed collagen I & IV, myofibroblast-like SMA- and vimentin-positive cells using immunohistochemistry, which suggested that this capsule was generated from host mesenchymal cells.⁵⁵ These findings are consistent with the present study results showing that the EPC capsule is enriched with collagen I.

In conclusion, EPC is surrounded with BM-like material resembling those surrounding some invasive tumour types and is significantly different from the BM of normal breast tissue and DCIS. This study provides further evidence that EPC is an indolent invasive carcinoma surrounded with BM-like material with biopathological features between *in situ* and invasive carcinoma on the basis of capsule characteristics. Most papillary tumours in different organs that are surrounded with BM-like material showed indolent behaviour with better prognosis; therefore, mechanisms that explain these phenomena should be further investigated.

Acknowledgements

We thank the Egyptian Ministry of Higher Education and Scientific Research and British Council who support SFG.

Author contributions

SFG stained and scored the cases with data analysis and interpretation and wrote the article draft and made critical revisions. CSR helped with microscopy examination and data interpretation and made critical revisions to the article. CA and NPM interpreted results and made critical revisions to the article. ER: conceived and planned the study, contributed to data interpretation, and made critical revisions to the article. All authors approved the final version.

Funding information

SFG is supported by and funded by the Egyptian Ministry of Higher Education and Scientific Research.

Ethical approval and consent to participate

This study obtained ethics approval for use the human tissue samples by the Northwest – Greater Manchester Central Research Ethics Committee under the title Nottingham Health Science Biobank (NHSB), reference number 15/NW/0685. Informed consent was obtained from all individuals and all samples were anonymised.

Conflict of interest

The authors declare that they have no conflicts of interest.

Data availability statement

The data that support the findings of this study are available from the corresponding author upon reasonable request.

References

1. Morgan S, Dodington D, Wu JM, Turashvili G. Solid papillary carcinoma and encapsulated papillary carcinoma of the breast: clinical-pathologic features and basement membrane studies of 50 cases. *Pathobiology* 2021; **88**: 359–373.
2. Tay TKY, Tan PH. Papillary neoplasms of the breast-reviewing the spectrum. *Mod. Pathol.* 2021; **34**: 1044–1061.
3. Rakha EA, Tun M, Junainah E, Ellis IO, Green A. Encapsulated papillary carcinoma of the breast: a study of invasion associated markers. *J. Clin. Pathol.* 2012; **65**: 710–714.
4. Rakha EA, Miligy IM, Goringe KL *et al.* Invasion in breast lesions: the role of the epithelial-stroma barrier. *Histopathology* 2018; **72**: 1075–1083.
5. Ghannam SF, Rutland CS, Allegrucci C, Mongan NP, Rakha E. Defining invasion in breast cancer: the role of basement membrane. *J. Clin. Pathol.* 2022; **76**: 11–18.
6. Barr LC. The encapsulation of tumours. *Clin. Exp. Metastasis* 1989; **7**: 277–282.
7. Barr LC, Carter RL, Davies AJS. Encapsulation of TUMOURS AS a modified wound healing response. *Lancet* 1988; **332**: 135–137.
8. Tan PH, Ellis I, Allison K *et al.* The 2019 World Health Organization classification of tumours of the breast. *Histopathology* 2020; **77**: 181–185.
9. Esposito NN, Dabbs DJ, Bhargava R. Are encapsulated papillary carcinomas of the breast in situ or invasive? A basement membrane study of 27 cases. *Am. J. Clin. Pathol.* 2009; **131**: 228–242.
10. Asgari M, Latifi N, Heris HK, Vali H, Mongeau L. In vitro fibrillogenesis of tropocollagen type III in collagen type I affects its relative fibrillar topology and mechanics. *Sci. Rep.* 2017; **7**: 1392.
11. Khalilgharibi N, Mao Y. To form and function: on the role of basement membrane mechanics in tissue development, homeostasis and disease. *Open Biol.* 2021; **11**: 200360.

12. Rodriguez-Teja M, Gronau JH, Breit C *et al*. AGE-modified basement membrane cooperates with Endo180 to promote epithelial cell invasiveness and decrease prostate cancer survival. *J. Pathol.* 2015; **235**: 581–592.
13. Fiore VF, Krajnc M, Quiroz FG *et al*. Mechanics of a multilayer epithelium instruct tumour architecture and function. *Nature* 2020; **585**: 433–439.
14. Drifka CR, Loeffler AG, Mathewson K *et al*. Comparison of Picrosirius red staining with second harmonic generation imaging for the quantification of clinically relevant collagen fiber features in histopathology samples. *J. Histochem. Cytochem.* 2016; **64**: 519–529.
15. Zunder SM, Gelderblom H, Tollenaar RA, Mesker WE. The significance of stromal collagen organization in cancer tissue: an in-depth discussion of literature. *Crit. Rev. Oncol. Hematol.* 2020; **151**: 102907.
16. Vogel B, Siebert H, Hofmann U, Frantz S. Determination of collagen content within picrosirius red stained paraffin-embedded tissue sections using fluorescence microscopy. *MethodsX.* 2015; **2**: 124–134.
17. Junqueira L, Cossermelli W, Brentani R. Differential staining of collagens type I, II and III by Sirius Red and polarization microscopy. *Arch. Histol. Jpn.* 1978; **41**: 267–274.
18. Liu J, Xu MY, Wu J *et al*. Picrosirius-polarization method for collagen fiber detection in tendons: a mini-review. *Orthop. Surg.* 2021; **13**: 701–707.
19. Rakha EA, Ahmed MA, Ellis IO. Papillary carcinoma of the breast: diagnostic agreement and management implications. *Histopathology* 2016; **69**: 862–870.
20. Xue M, Jackson CJ. Extracellular matrix reorganization during wound healing and its impact on abnormal scarring. *Adv. Wound Care (New Rochelle).* 2015; **4**: 119–136.
21. Iorio V, Troughton LD, Hamill KJ. Laminins: roles and utility in wound repair. *Adv. Wound Care (New Rochelle).* 2015; **4**: 250–263.
22. Rakha EA, Gandhi N, Climent F *et al*. Encapsulated papillary carcinoma of the breast: an invasive tumor with excellent prognosis. *Am. J. Surg. Pathol.* 2011; **35**: 1093–1103.
23. Nicolas MM, Wu Y, Middleton LP, Gilcrease MZ. Loss of myoepithelium is variable in solid papillary carcinoma of the breast. *Histopathology* 2007; **51**: 657–665.
24. Mulligan AM, O'Malley FP. Metastatic potential of encapsulated (intracystic) papillary carcinoma of the breast: a report of 2 cases with axillary lymph node micrometastases. *Int. J. Surg. Pathol.* 2007; **15**: 143–147.
25. Fayanju OM, Ritter J, Gillanders WE *et al*. Therapeutic management of intracystic papillary carcinoma of the breast: the roles of radiation and endocrine therapy. *Am. J. Surg.* 2007; **194**: 497–500.
26. Lefkowitz M, Lefkowitz W, Wargotz ES. Intraductal (intracystic) papillary carcinoma of the breast and its variants: a clinicopathological study of 77 cases. *Hum. Pathol.* 1994; **25**: 802–809.
27. Solorzano CC, Middleton LP, Hunt KK *et al*. Treatment and outcome of patients with intracystic papillary carcinoma of the breast. *Am. J. Surg.* 2002; **184**: 364–368.
28. Wynveen CA, Nehozina T, Akram M *et al*. Intracystic papillary carcinoma of the breast: an in situ or invasive tumor? Results of immunohistochemical analysis and clinical follow-up. *Am. J. Surg. Pathol.* 2011; **35**: 1–14.
29. Golestani R, Singh K, Karam P *et al*. Significance of myoepithelial cell layer in breast ductal carcinoma in situ with papillary architecture with and without associated invasive carcinoma. *Clin. Breast Cancer* 2022; **23**: 91–100.
30. Akladios CY, Roedlich MN, Bretz-Grenier MF, Croce S, Mathelin C. Intracystic papillary carcinoma of the breast: a diagnostic challenge with major clinical impact. *Anticancer Res* 2014; **34**: 5017–5020.
31. Cserni G. "Revertant" mammary solid papillary carcinoma in lymph node metastasis. *Pathol. Oncol. Res.* 2002; **8**: 74–77.
32. Pervez S, Khan H. Infiltrating ductal carcinoma breast with central necrosis closely mimicking ductal carcinoma in situ (comedo type): a case series. *J Med Case Reports* 2007; **1**: 83.
33. Li X, Xu Y, Ye H, Qin S, Hou F, Liu W. Encapsulated papillary carcinoma of the breast: a clinicopathological study of 49 cases. *Curr. Probl. Cancer* 2018; **42**: 291–301.
34. Pisanu A, Deplano D, Reccia I, Porceddu G, Uccheddu A. Encapsulated papillary thyroid carcinoma: is it a distinctive clinical entity with low-grade malignancy? *J. Endocrinol. Invest.* 2013; **36**: 78–83.
35. Carcangiu ML, Zampi G, Pupi A, Castagnoli A, Rosai J. Papillary carcinoma of the thyroid. A clinicopathologic study of 241 cases treated at the University of Florence, Italy. *Cancer* 1985; **55**: 805–828.
36. Ito Y, Hirokawa M, Urano T *et al*. Biological behavior and prognosis of encapsulated papillary carcinoma of the thyroid: experience of a Japanese hospital for thyroid care. *World J. Surg.* 2008; **32**: 1789–1794.
37. Evans HL. Encapsulated papillary neoplasms of the thyroid. A study of 14 cases followed for a minimum of 10 years. *Am. J. Surg. Pathol.* 1987; **11**: 592–597.
38. Schröder S, Dralle H, Rehpenning W, Böcker W. Prognostic criteria of papillary thyroid cancer. Morphologic clinical analysis of 202 cases of tumor. *Langenbecks Arch. Chir.* 1987; **371**: 263–280.
39. Piana S, Frasoldati A, Di Felice E *et al*. Encapsulated well-differentiated follicular-patterned thyroid carcinomas do not play a significant role in the fatality rates from thyroid carcinoma. *Am. J. Surg. Pathol.* 2010; **34**: 868–872.
40. Bai Y, Kakudo K, Li Y *et al*. Subclassification of non-solid-type papillary thyroid carcinoma identification of high-risk group in common type. *Cancer Sci.* 2008; **99**: 1908–1915.
41. Bayadsi H, Barghout G, Gustafsson M, Sund M, Hennings J. The expression of stromal biomarkers in small papillary thyroid carcinomas. *World J. Surg. Oncol.* 2022; **20**: 340.
42. Rich NE, Singal AG. Overdiagnosis of hepatocellular carcinoma: prevented by guidelines? *Hepatology* 2022; **75**: 740–753.
43. Grigioni WF, D'Errico A, Mancini AM *et al*. Hepatocellular carcinoma: expression of basement membrane glycoproteins. An immunohistochemical approach. *J. Pathol.* 1987; **152**: 325–332.
44. Grigioni WF, D'Errico A, Biagini G *et al*. The capsule surrounding primary liver tumors: wherefrom its prognostic significance? *Int. J. Cancer* 1990; **45**: 637–643.
45. Torimura T, Ueno T, Inuzuka S, Tanaka M, Abe H, Tanikawa K. Mechanism of fibrous capsule formation surrounding hepatocellular carcinoma. Immunohistochemical study. *Arch. Pathol. Lab. Med.* 1991; **115**: 365–371.
46. Gulubova MV. Collagen type III and type IV detection in and around human hepatocellular carcinoma. *Gen. Diagn. Pathol.* 1997; **142**: 155–163.
47. Dehan P, Waltregny D, Beschin A *et al*. Loss of type IV collagen alpha 5 and alpha 6 chains in human invasive prostate carcinomas. *Am. J. Pathol.* 1997; **151**: 1097–1104.
48. Chen W-J, Pan C-C, Shen S-H *et al*. Clear cell papillary renal cell carcinoma – An indolent subtype of renal tumor. *J. Chin. Med. Assoc.* 2018; **81**: 878–883.

49. Roquero L, Kryvenko ON, Gupta NS, Lee MW. Characterization of fibromuscular pseudocapsule in renal cell carcinoma. *Int. J. Surg. Pathol.* 2015; **23**: 359–363.
50. Gatalica Z, Miettinen M, Kovatich A, McCue PA. Hyaline globules in renal cell carcinomas and oncocytomas. *Hum. Pathol.* 1997; **28**: 400–403.
51. Ninomiya Y, Kagawa M, Iyama K-i et al. Differential expression of two basement membrane collagen genes, COL4A6 and COL4A5, demonstrated by immunofluorescence staining using peptide-specific monoclonal antibodies. *J. Cell Biol.* 1995; **130**: 1219–1229.
52. de Riese W, Allhoff EP, Liedke S et al. *Investigation of the Tumor Capsule in Renal Cell Carcinoma and Its Significance for Treatment. Contemporary Research on Renal Cell Carcinoma.* Berlin, Heidelberg: Springer Berlin Heidelberg, 1994.
53. Lohi J, Korhonen M, Leivo I et al. Expression of type IV collagen alpha1(IV)-alpha6(IV) polypeptides in normal and developing human kidney and in renal cell carcinomas and oncocytomas. *Int. J. Cancer* 1997; **72**: 43–49.
54. Tan YQ, Tay WK, Ooi LY, Thamboo TP, Tiong HY. Multiphoton microscopic study of the renal cell carcinoma Pseudocapsule: implications for tumour enucleation. *Urology* 2020; **144**: 249–254.
55. Stamatou K, Kostakos E, Labrakopoulos A, Tepelenis N, Zizi-Serbetzoglou A. The fibrous capsule (pseudocapsule) in renal clear cell carcinoma (RCCC). *Virchows Arch.* 2009; **455**: S1–S482.